Electrical conductivity and chemical diffusivity of NiAl₂O₄ spinel under internal reforming fuel cell conditions[†]

L. KOU and J.R. SELMAN
Department of Chemical and Environmental Engineering, Illinois Institute of Technology, 10 W. 33rd St.,
Chicago, IL 60616, USA

Abstract

NiAl₂O₄ spinel was formed by solid state reaction. Its electrical conductivity was measured in the temperature range of 680–940 °C and under various oxygen-rich environments, as well as under reducing conditions. From the temperature dependence of the conductivity, the activation energies for conduction increase for decreasing oxygen partial pressures. From the partial oxygen pressure dependence, the defect structure of the material was analysed. The conductivity change with respect to P_{O_2} can be attributed to singly and doubly ionized nickel vacancies. The chemical diffusivity of the oxide was determined by conductivity relaxation upon abrupt change in P_{O_2} in the surrounding atmosphere. The oxygen chemical diffusion coefficient is of the order of magnitude of 10^{-4} cm^2 s^{-1}.

1. Introduction

Oxides with mixed electronic and oxygen ionic conductivities have been widely studied for use as components in high temperature fuel cells. Nickel aluminate spinel has been proposed as a candidate material for IR–SOFC anodes because it exhibits 'autogenerated catalysis' for methane steam reforming under reducing conditions [1]. As a candidate electrode material, its physical properties, especially electrical conductivity and chemical diffusivity, are of special interest.

In this study we present the results of a determination of conductivity and oxygen diffusion coefficient of NiAl₂O₄ spinel.

1.1. Electrical conductivity

The electrical conductivity of a flat sample of arbitrary shape can be measured by the van der Pauw four-point method [2]. The specific resistivity of the sample depends on two-point voltage differences as expressed in Equation 1:

$$\rho = \frac{\pi d}{\ln 2} \frac{(R_{AB,CD} + R_{BC,DA})}{2} f\left(\frac{R_{AB,CD}}{R_{BC,DA}}\right) \qquad (1)$$

where $R_{AB,CD}$ is defined as the voltage difference between points C and D per unit current passing through points A and B. A similar definition applies to $R_{BC,DA}$. f is a tabulated factor.

From the temperature dependence of the conductivity, the activation energy of conduction can be determined for different partial oxygen pressures. From the partial oxygen pressure dependence, the defect model is established.

1.2. Chemical diffusivity

In chemical relaxation experiments, an abrupt change of chemical potential of one of the constituent elements, usually P_{O_2} for oxide samples, is imposed on a sample under constant temperature, and the change with time of the physical property such as weight or volume of the sample is pursued until a new thermodynamica equilibrium state is reached. Because electrical conductivity is much more sensitive to change of oxygen chemical potential in the atmosphere than other properties such as weight, considerable changes in conductivity can be observed even when the P_{O_2} change of the corresponding nonstoichiometry is very small. Chemical diffusion coefficients in many oxides have been determined by this method [3–7].

Relaxation experiments were conducted in which the change of electrical conductivity after a sudden change of P_{O_2} in the surrounding atmosphere was monitored as a function of time. The transient behaviour in the reequilibration process was analysed by fitting the relaxation data to the solution of Fick's second law of diffusion, Equation 2, with appropriate boundary conditions:

[†] Dedicated to the memory of Daniel Simonsson

$$\frac{\sigma_{app}(t) - \sigma_{app}(0)}{\sigma_{app}(\infty) - \sigma_{app}(0)} = 1 - \sum_{n=1}^{\infty} \frac{8}{(2n+1)^2 \pi^2}$$
$$\times \exp\left(-\frac{(2n+1)^2 \pi^2 Dt}{4L^2}\right) \quad (2)$$

The chemical diffusion coefficient for both oxidation and reduction runs will be reported here.

2. Experimental details

2.1. *Sample preparation*

Nickel aluminate spinel was formed from raw material $NiO + \alpha\text{-}Al_2O_3$ by mechanical ball milling, pressing, and solid state reaction. After formation, the sample was polished on both sides to make certain that it had uniform thickness. Four 0.01 inch diameter Pt wires were connected to different points on the sample circumference by means of Pt paste. The sample was cured at 600 °C overnight before the measurement.

2.2. *Set-up*

The schematic of the experimental set-up is shown in Figure 1. It is composed of a quartz gas liner, an inlet gas mixer, an EG&G model 173 potentiostat/galvanostat, and an Omega data acquisition system. Two of the Pt wires were connected to the galvanostat, which was used to supply constant current to the sample. The other two Pt wires were connected to the Omega data acquisition system, which was used to record the corresponding voltage change. The temperature of the sample was controlled by the electric furnace. The gas atmosphere around the sample was controlled by adjusting the inlet gas composition through the gas mixer.

Air and Ar were supplied to the system to control the oxidizing gas environment inside the gas liner. When reducing environment was desired, pure H_2 was supplied to the sample, and it was reduced first under pure H_2 at 600 °C for 12 h, after which the measurement was carried out.

To minimize the effect of thermal emf between the potential probes, voltages were measured for two different levels of current, and the resistance was determined from the slope of the current–potential plot.

The set-up was used for both electrical conductivity and chemical diffusivity measurement.
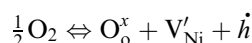
3. Results and discussion

3.1. *Electrical conductivity*

Results of temperature and P_{O_2} dependent electrical conductivity are shown in Figures 2 and 3, respectively. In Figure 2, from the slope and intercept of the fitted line, the expressions for electrical conductivity under various partial oxygen pressures are extrapolated as shown in Table 1.

From Figure 3, which is the conductivity partial oxygen pressure dependence, we can see experimentally that conductivity is proportional to the partial oxygen pressure to the order of $0.207 \sim 0.25$. This is in agreement with the defect structure analysed below. The defect model is proposed as
Model I:

$$\frac{1}{2}O_2 \Leftrightarrow O_o^x + V_{Ni}' + \dot{h}$$

The equilibrium constant is

$$K1 = \frac{[O_o^x][V_{Ni}'][\dot{h}]}{P_{O_2}^{1/2}} \quad (3)$$
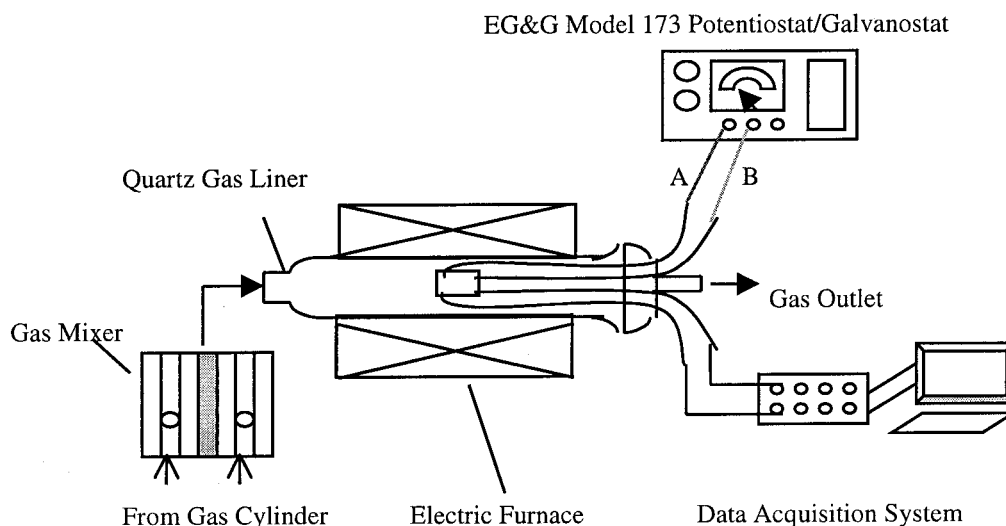
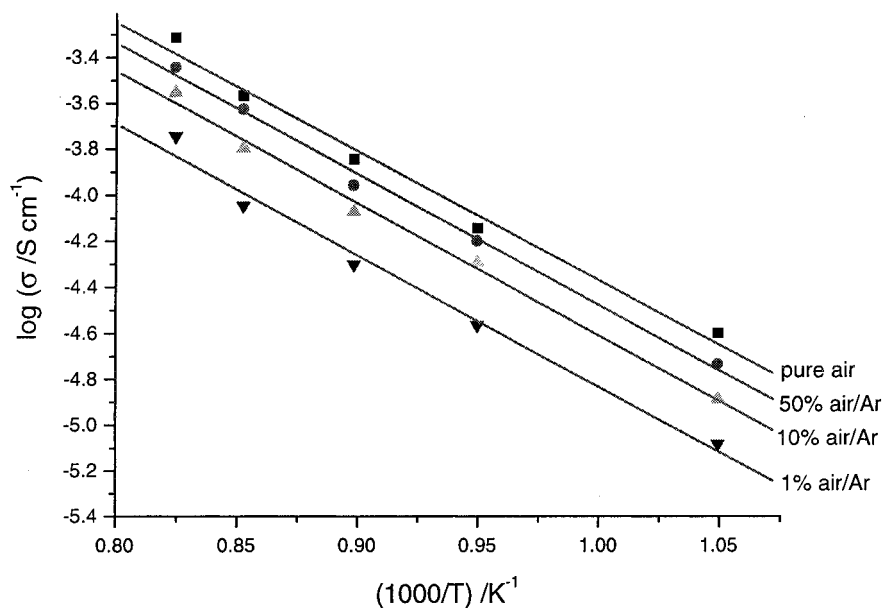EG&G Model 173 Potentiostat/Galvanostat

Fig. 1. Experimental set-up.

Fig. 2. Electrical conductivity–temperature dependence. Data (σ_o/S cm^{-1}, E_A/kJ mol^{-1}): pure air (17.05, 107.21); 50% air (16.3, 108.9); 10% air (13.36, 109.1); 1% air (7.36, 109.76).
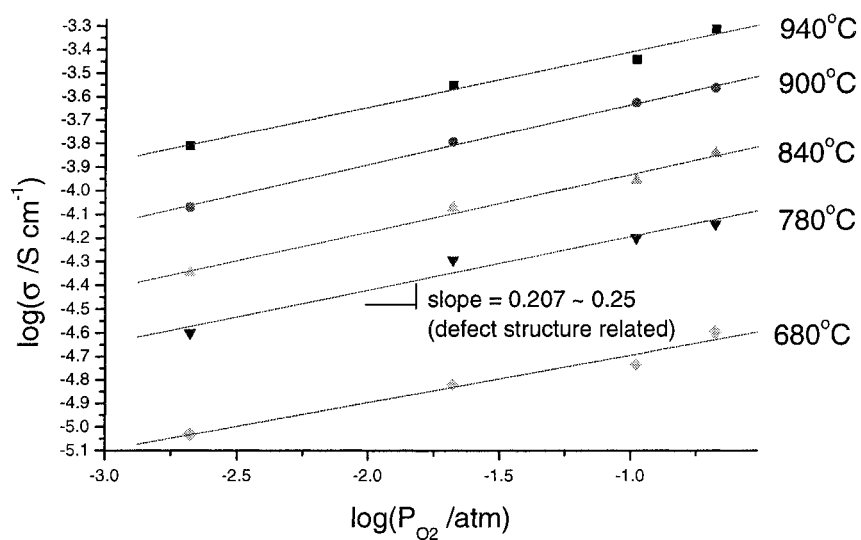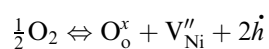

Fig. 3. Electrical conductivity–partial oxygen pressure dependence.

charge balance:

$$[V'_{Ni}] = [\dot{h}] \tag{4}$$

$$\sigma \propto [V'_{Ni}] \propto P_{O_2}^{1/4}$$

Model II:

$$\tfrac{1}{2}O_2 \Leftrightarrow O_o^x + V''_{Ni} + 2\dot{h}$$

The equilibrium constant is

$$K2 = \frac{[O_o^x][V''_{Ni}][\dot{h}]^2}{P_{O_2}^{1/2}} \tag{5}$$

charge balance:

$$2[V''_{Ni}] = [\dot{h}] \tag{6}$$

$$\sigma \propto [V''_{Ni}] \propto P_{O_2}^{1/6}$$

Table 1. Electrical conductivity of NiAl$_2$O$_4$: partial oxygen pressure dependency

P_{O_2}/atm	σ/S cm^{-1}
0.21	17.05 exp(−107210/RT)
0.105	16.3 exp(−108900/RT)
0.021	13.3 exp(−109100/RT)
0.0021	7.36 exp(−109760/RT)

These defect structure models are both in reasonable agreement with the experimental result. Therefore, we can conclude that the conductivity is due to the presence of both singly and doubly ionized nickel vacancies.

Electrical conductivity measurement was performed under pure H_2 environment also. Results are shown in Figure 4. The expression for the Arrhenius equation is as follows:
Pure H_2:

$$\sigma = 1.57 \times 10^{-5} \exp(-10414/RT)$$

where σ is in S cm^{-1}.

The conductivity was not improved after reduction. This is probably because the nickel metallic conduction path formed after reduction is not continuous.

3.2. Chemical diffusivity

A typical example of the change of conductivity of NiAl$_2$O$_4$ is shown in Figure 5. Relaxation data were analysed by a nonlinear least-squares fitting to the solution of Fick's second law (Equation 2). The oxygen chemical diffusion coefficients determined are shown in Figure 6 for redox processes.

In Figure 5, there is a slight difference in time constants needed to adjust equilibrium states of processes (I) and/ or (II). This slight difference may be due to different rate-limiting steps in the reequilibration process [8].

From Figure 6, chemical diffusion coefficients are determined for both reduction and oxidation processes according to (I) and/or (II) between air and 1% air/Ar. The Arrhenius relation can be expressed as

$$D_{\text{red}} = 9.13 \times 10^{-3} \exp(-32440/RT)$$

$$D_{\text{oxid}} = 6.15 \times 10^{-2} \exp(-55950/RT)$$

where D_{red} and D_{oxid} are in cm^2 s^{-1}. These diffusivities, which are quite high for a solid-state process, are apparently those of oxide ions and/or nickel vacancies created according to model (I) and/or (II).
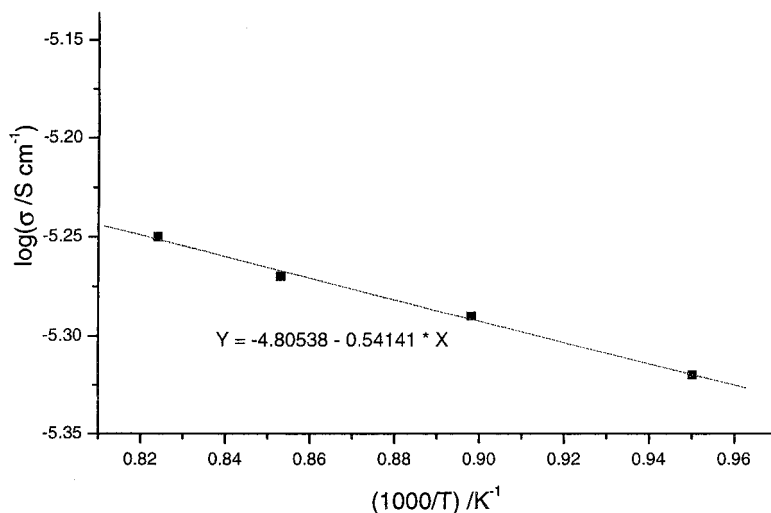

Fig. 4. Electrical conductivity under H_2 environment–temperature dependence. Conditions: $\sigma_o = 1.57 \times 10^{-5}$ S cm^{-1}; $E_A = 10.414$ kJ mol^{-1}.
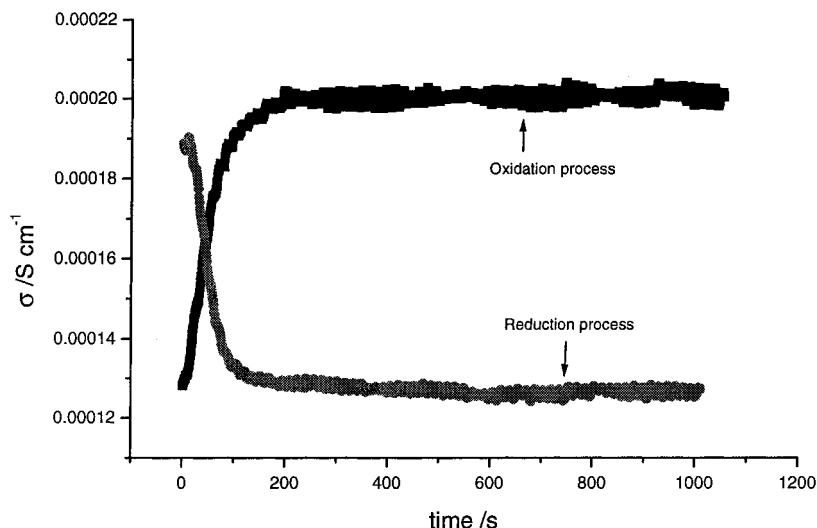

Fig. 5. Change of conductivity as a function of time for NiAl$_2$O$_4$ while switching gas atmosphere from air to 1% air/Ar at 940 °C.
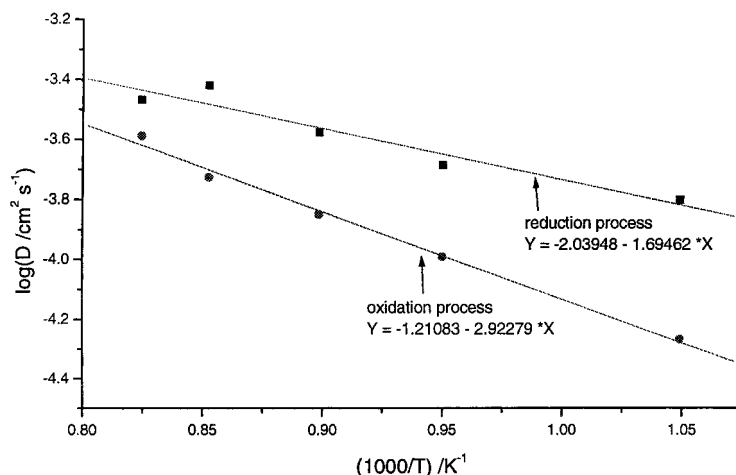
Fig. 6. Chemical diffusion coefficient of oxygen in NiAl$_2$O$_4$ upon transition from air to 1% air/Ar–temperature dependence. $D_{red} = 9.13 \times 10^{-3}$ exp($-32440/RT$) cm^2 s^{-1}; $D_{oxid} = 6.15 \times 10^{-2}$ exp($-55950/RT$) cm^2 s^{-1}.

4. Conclusion

The electrical conductivity of NiAl$_2$O$_4$ spinel was determined by the van der Pauw four-point method. It is a p-type semiconductor. The activation energies for electrical conduction have been extrapolated. The associated defect structure of the material has been analyzed. The data suggest that the conductivity is due to the simultaneous presence of singly and doubly ionized nickel vacancies.

The chemical diffusion coefficient of oxygen in NiAl$_2$O$_4$ was determined by the conductivity relaxation method with abrupt change in the gas environment between air and 1% air/Ar. The diffusion coefficient increases with increasing temperature. At 940 °C, the oxide chemical diffusion coefficient is

$$D_{red} = 3.66 \times 10^{-4}$$

$$D_{oxid} = 2.40 \times 10^{-4}$$

where D_{red} and D_{oxid} are in cm^2 s^{-1}. This is in agreement with Figure 5, which shows a slightly shorter time for the reduction process to reach equilibrium, than for the oxidation process.

References

1. L. Kou and J.R. Selman, VI International Symposium on 'solid oxide fuel cells', 196th ECS meeting, Honolulu (1999).
2. L.J. van der Pauw, *Philips Res. Repts.* **13** (1958) 1–9.
3. L.C. Walters and R.E. Grace, *J. Phys. Chem. Solids.* **28** (1967) 245.
4. K. Kitazawa and R.L. Coble, *J. Am. Ceram. Soc.* **57** (1974) 250.
5. R. Wernicke, *Philips Res. Repts.* **31** (1976) 526.
6. R. Farhi and G. Petot-Ervas, *J. Phys. Chem. Solids.* **39** (1978) 1169.
7. C.J. Yu, D.M. Sparlin and H.U. Anderson, *J. Am. Ceram. Soc.* **70** (1987) C189.
8. J. Nowotny, J. Oblakowski, A. Sadowski, and J.B. Wagner, Jr., *Oxid. Met. (USA)* **14**(5) (1980) 437.